Supercritical water gasification of RDF and its components over RuO_2/γ-Al_2O_3 catalyst: new insights into RuO_2 catalytic reaction mechanisms

Jude. A. Onwudili[*]

Chemical Engineering & Applied Chemistry,
School of Engineering & Applied Science
Aston University, Aston Triangle, Birmingham, B4 7ET, United Kingdom

Abstract

Five samples, including a composite refuse derived fuel (RDF) and four combustible components of municipal solid wastes (MSW) have been reacted under supercritical water conditions in a batch reactor. The reactions have been carried out at 450 °C for 60 min reaction time, with or without 20 wt% RuO_2/gamma-alumina catalyst. The reactivities of the samples depended on their compositions; with the plastic-rich samples, RDF and mixed waste plastics (MWP), giving similar product yields and compositions, while the biogenic samples including mixed waste wood (MWW) and textile waste (TXT) also gave similar reaction products. The use of the heterogeneous ruthenium-based catalyst gave carbon gasification efficiencies (CGE) of up to 99 wt%, which was up by at least 83% compared to the non-catalytic tests. In the presence of RuO_2 catalyst, methane, hydrogen and carbon dioxide became the dominant gas products for all five samples. The higher heating values (HHV) of the gas products increased at least two-fold in the presence of the catalyst compared to non-catalytic tests. Results show that the ruthenium-based catalyst was active in feedstock steam reforming, methanation and possible direct hydrogenolysis of C-C bonds. This work provides new insights into the catalytic mechanisms of RuO_2 during SCWG of carbonaceous materials, along with the possibility of producing high yields of methane from MSW fractions.

Keywords: MSW, supercritical water gasification, ruthenium catalysis, mechanisms, methane

* Corresponding Author.
Tel.: +44 121 204 4703
Email address: j.onwudili@aston.ac.uk

1.0. Introduction

Rapid urbanization and technological developments are largely responsible for the increasing generation of millions of tonnes of municipal solid wastes (MSW) in major cities around the world. MSW can be broadly classified into organic and inorganic fractions. Among the organic components of MSW, further classifications can be made into biodegradable and non-biodegradable fractions. By far, food and garden wastes occupy a huge proportion of MSW but these are biodegradable and are often treated by anaerobic digestion (AD) to produce biogas, leading to complete mineralization. After the separation of recyclables, the mixture of non-readily biodegradable organic components make up a combustible fraction of MSW, which can be made into solid recovered fuels (SRF) and refuse derived fuels (RDF), depending on the specification. The stringent regulations concerning the production and utilization of SRF and RDF indicate that many components of MSW cannot be directly burned as fuels [1-2]. Mass-produced synthetic polymers such as plastics and textile materials fall into the category of combustible MSW fractions [3]. Other organic components of MSW that do not hold huge attractions for AD operators include waste wood and reinforced cardboards.

Advanced thermochemical technologies suitable for treating plastics and other combustible organic wastes and materials include incineration, pyrolysis and gasification. These technologies convert organic wastes to three products namely; gas, liquid (oil) and solid residues (mainly char) [3]. The relative proportions of the products depend mostly on the type of technology, the reaction conditions and presence of catalysts or additives. Incineration is a limited technology in terms of its products, which include electricity, heat and bottom ash. Gasification produces syngas ($CO + H_2$) as the main product, which offers the flexibility for use as fuel or chemical building blocks but in general the gas products are composed of hydrogen, CO, CO_2, methane, and C_2-C_4 hydrocarbon gases. Pyrolysis can be designed to produce oils (fast pyrolysis) or to produce char (slow pyrolysis) as the main product. However, pyrolysis and gasification require dry feedstock, which may add to the costs of processing high-moisture MSW wastes due to the need for a drying or dewatering stage.

Supercritical water gasification (SCWG) is the technology of choice for wet organic feedstocks [4-6]. Wet solid wastes with combustible components such as medical wastes, sludges and fines from mechanical-biological treatment (MBT) plants can be treated using SCWG technology without the need for further drying. The technology can, however also be used for

the conversion of dry organic wastes and materials, where the addition of water is justified since supercritical water serves as both reaction medium and reactant. It has been shown that the mechanism for hydrogen formation during SCWG is mainly through the formation of CO, followed by the water-gas shift reaction (WGSR) of the CO [7-9]. In addition, methane formation in SCWG would usually involve demethylation but methanation of CO or CO_2 using the *in situ* produced hydrogen from the WGSR has been reported as equally important. Furthermore, there has been evidence of proton-deuterium exchanges during organic chemical reactions in supercritical water using deuterated water (D_2O) as reaction medium [10]. More recently, Park and Tomiyasu [11] used D_2O as the reaction medium during SCWG of biomass and found that the hydrogen atoms in the hydrogen gas and methane obtained from the reactions were deuterium, indicating that D_2O supplied the hydrogen atoms in the gasification products. Hence, water is an important reagent during hydrothermal gasification and so the application of SCWG to otherwise 'dry' feedstock can be advantageous in terms of selectivity and specificity of gas components.

Literature shows that plastics and other solid non-biodegradable organic wastes have been successfully processed under hydrothermal conditions. Hydrothermal processes for plastics include depolymerization of condensation polymers such as polyurethane, nylon, Teflon and waste fibre reinforced thermoset plastics to obtain monomeric compounds [12]. In addition, SCWG of waste plastics and model plastic materials [13-14] as well as plastics/biomass mixtures [15] has been investigated by several groups in the last decade. One of the advantages of SCWG is that it can produce clean, pressurized combustible gas products, making post-production use easier. Therefore, the application of SCWG for the processing of combustible fractions of MSW can be accomplished in an environmental friendly way.

Application of catalysts during SCWG of organic materials can considerably enhance gasification efficiency and product selectivity. In particular, nickel and ruthenium catalysts have shown good selectivities for hydrogen and/or methane during SCWG [16-17]. Ruthenium and ruthenium oxide have shown excellent promise for gasification of biomass and even plastic-rich sludges [17]. In this present study, SCWG of non-biodegradable solid organic fractions of MSW, essentially the components of RDF, has been investigated in the presence of RuO_2/γ-Al_2O_3 catalyst. Ruthenium is a well-known catalyst for C-C bond cleavages in organic compounds and can promote methanation reactions as well as WGS reactions for methane and hydrogen production, respectively [16-19]. Methane and hydrogen are two of the

cleanest energy carriers and the infrastructures from their distribution and utilization already exists and so do their markets. The MSW fractions include mixed waste plastics, mixed waste wood, waste textiles, trommel fines and RDF. The novelty of catalytic SCWG of MSW fractions is the direct utilization of intractable wet carbonaceous feedstocks for the production of clean fuel gases in high yields. In addition, this work would provide new insights into the catalytic mechanisms of RuO_2 during SCWG of different carbonaceous wastes, which would contribute to future process development efforts. The aim of the study was to investigate the feasibility of producing synthetic methane and hydrogen from these fractions of MSW in a batch reactor via SCWG.

2.0 Experimental

2.1. Materials

Combustible fractions of MSW were obtained from a household materials recycling facility (MRF) in Skegness, UK. These included mixed wastes plastics (MWP), mixed waste wood (MWW), waste textiles (TXT) and trommel fines (TF) and a composite RDF sample. The photographs of the different fractions in their original forms and after pulverizing using a cryogenic mill are shown in the *Supplementary Information*. In each case, the feedstocks were sampled by taking equal mass of each of the items in each sample to make a composite sample of 5.0 g each. Each 5.0 g composite sample was pulverized using a Cryogenic Mill and sieved to ≤200 μm. The pulverized samples were used for sample characterization and for the SCWG process. The elemental (CHNS) compositions of the samples were determined using a Carlo Erba Flash EA 1112 compact analyser. Table 1 shows the number of individual items within each sample as well as the proximate (as-received basis) and ultimate (dry-ash-free basis) compositions of the samples. The proximate analyses of the samples were performed using a Metler Toledo TGA/DSC 1 Star System. Depending on the density of the samples, approximately between 10 – 14 mg was loaded into the sample pan and heated under nitrogen atmosphere (50 ml min^{-1}) from 20 °C to 105 °C at a constant rate of 25 °C min^{-1} and held for 10 min at 105 °C. Then the temperature was ramped to 900 °C at the same heating rate and held for 10 min at 900 °C. Thereafter, air was introduced at this temperature and this final conditions held for a further 15 min. Figure 1 shows the TGA/DTG profiles of the samples. Commercial ruthenium oxide – gamma alumina (RuO_2/γ-Al_2O_3) catalyst containing 20 wt% RuO_2, obtained from Catal Ltd, a UK-based SME was used in these tests. The catalyst was in the form of 3 mm diameter pellets but was pulverized and sieved to ≤125 μm particle size before use, in order to increase the catalyst-feed contact surface in the non-stirred reactor.

4

Briefly, the pulverized catalyst had a BET surface area of 7.97 $m^2 g^{-1}$, a pore volume of 0.025 $cm^3 g^{-1}$, nominal RuO_2 and ruthenium metal contents of 20 wt% and 15.1 wt%, respectively.

2.2. Methods

In each case, 17 ml of deionized water was added into a cylindrical 75 ml Hastelloy reactor, followed by 1.0 g of the 20 wt% RuO_2/γ-Al_2O_3 catalyst. Detailed description of the batch hydrothermal reactor, which is rated up to 650 °C and 45 MPa has been published earlier [20]. The catalyst and water were mixed with a glass rod before 2.0 g of the feed was loaded. The reactor was sealed and purged with nitrogen gas for 10 min to exclude air. Afterwards, the reactor was pressurized to 1 bar with nitrogen gas prior to heating. The sealed reactor was placed in a 1.5 kW ceramic knuckle heater. A thermocouple placed in a thermowell at the bottom of the reactor was used to monitor the temperature inside the reactor. The reactor heat-up time to reach the designated temperature of 450 °C was 12 min, which indicated that the reactor was heated at an average rate of 21 °C min^{-1} to this temperature where it was held for a further 60 min. At the end of the experiment, the reactor was withdrawn from the heater and cooled quickly with compressed air to room temperature, reaching 50 °C after 5 min. The gas products were sampled using gas-tight plastic syringes for further analysis.

2.3. Gas Analysis

The gas products were analysed offline by a system of three gas chromatographs (GCs), with already published analytical conditions [20-21]. One of the GC was fitted with a 2 m x 2 mm Molecular Sieve column for the separation of hydrogen, oxygen, nitrogen and CO, which were detected by a thermal conductivity detector (TCD). CO_2 was analysed on a 2 m x 2 mm Hysesp column and detection was also by TCD. Hydrocarbon gases from $C_1 - C_4$ were separated on another 2 m x 2 mm Hysesp column and detected by a flame ionization detector (FID). The analytical conditions used for the GC and detectors. Each gas sample was analysed 2-3 times and the averages used in calculations. The gas compositions were obtained in volume percent from the GCs and these were used to calculate the moles of each component using the Ideal Gas Law and Henry's Law. Standard deviations of less than 2% in gas compositions were obtained during replicate injections of the same gas samples. Yields of each gas component was calculated in mol kg^{-1} of feed as follows;

$$\text{Gas component Yield (mol kg}^{-1}) = \frac{\text{moles of gas obtained from GC analysis}}{\text{mass of feed used in kg}}$$

2.4. Sampling of reactor contents

On completion of gas analyses, the remaining gas was vented and the reactor opened to sample the solid and liquid residuals. At first, the reactor residuals (liquid and solid) were poured into a clear glass bottle and 5 ml of the liquid fraction withdrawn for total organic carbon (TOC) analysis. Furthermore, the reactor was rinsed thoroughly with dichloromethane (DCM) and added to the same glass bottle. In this study, 15 ml or 30 ml of DCM were used for the residuals from catalytic tests and non-catalytic tests, respectively due to the observed yields of oil products. Aliquots of the DCM were carefully used to rinse out the reactor. Thereafter, the solid and liquid fractions were separated by vacuum filtration, using additional DCM (15 ml each) to wash the solid residues.

2.5. Liquid analyses

The TOC contents of the liquid products were determined in two different ways. First, the mixed samples initially withdrawn from the reactor were analysed for TOC using a HACH IL 550 TOC-TN TOC analyser. Second, the liquid product mixed with DCM was transferred into a separating flask, agitated and allowed to stand for 30 min in order to separate into organic (DCM and oil) and aqueous phases. Then, the organic fraction was drawn off. Additional 10ml of DCM was used to ensure quantitative extraction of the DCM-soluble organics. The resulting aqueous layer was left open overnight in a fume hood to allow any entrained DCM to slowly evaporate off. At the same time, aqueous-layer controls were prepared by adding 15 ml or 30 ml of DCM to deionized water and following the same procedure for the oil extraction. The aqueous phases were subsequently analysed using the TOC analyser described above. Both controls gave TOC values <40 mgC L^{-1}, indicating minimal contributions of any leftover DCM to TOC values in the aqueous layers.

Results of the TOC analyses from the liquid product sampled directly (not extracted) from the reactor were expectedly much higher than those obtained from the analyses of the extracted aqueous layers. More importantly however, the TOC results from the non-extracted phase varied widely, giving average standard deviation of about 25%, while the latter much more consistent with standard deviations of $\leq 4.2\%$. These results showed that it was difficult to obtain reliable TOC values from the mixed liquid products without an initial solvent extraction step to separate the aqueous and organic phases. Hence, the TOC values of the extracted aqueous layers were used in this study.

2.6. Solid Analysis

The recovered solid residues were dried in an oven at 105 °C for 2 h and then homogenized with a laboratory mortar and pestle before further analysis. The char contents of the recovered residues were determined via temperature-programmed oxidation using a Stanton-Redcroft thermogravimetric analyser (TGA) interfaced with a Nicolet Magna IR-560 FT-IR. Furthermore, the CHNSO composition of the solid residues were determined using the same elemental analyser mentioned earlier in Section 2.1. In addition, the fresh catalyst, the used non-calcined catalyst (as recovered and dried) and the used calcined catalyst were all analysed by X-ray diffraction (XRD) (Bruker D8) with Cu Ka radiation for the presence of crystalline substances including ruthenium oxide and alumina. Furthermore, these solid samples were also characterised using Jeol JSM-6610LV Scanning Electron Microscope coupled to an Oxford Instruments INCA X-max80 EDX system (SEM-EDX). The detailed description and use of these instruments have been published earlier [22].

2.7. Material (carbon) balance calculations

Supercritical water has been shown to contribute oxygen and hydrogen to gas products during SCWG [17, 23]. Indeed in this work, the mass of gas products during catalytic runs with the ruthenium catalyst were significantly higher than the mass of the feedstock loaded into the reactor. For example, during the SCWG of 2.0 g mixed wastes plastics, 3.21 g of gas products were obtained, which amounted to a 1.6 times increase in mass, mainly due to the formation of carbon dioxide from a predominantly low-oxygen feedstock (Table 1).Therefore, due to the participation of water in the SCWG process, the materials balance in this work has been reported in terms of carbon balance, since the feedstocks were the only source of carbon in this work. The results from gas analysis were used to calculate the weight percent of carbon in the carbon-containing gas products i.e. CO, CO_2 and the (C_1-C_4) hydrocarbon gases. The TOC results accounted for the carbon contents in the aqueous fractions, while the CHNSO analyses provided the carbon contents in the solid residues. The carbon contents of the oil products were obtained by difference.

3.0. Results and Discussions

3.1. Carbon balance

Following the analyses above, the carbon distribution into gas products, aqueous residuals and solid residues were calculated based on the percentage composition of carbon in each feed, using the following equation;

$$Carbon\ distribution, \% = \frac{Mass\ of\ carbon\ in\ a\ reaction\ product\ (g)\ x\ 100}{Mass\ of\ carbon\ in\ feed\ (g)}$$

The carbon balances in Table 2 have been normalized to 100% on the assumption that, by accurately determining the carbon contents in the gas, solid and aqueous fractions above, then the balance carbon could only be in the oil products. It can be seen from Table 2 that during the non-catalytic experiments, a large proportion of the feed-carbon atoms remained in the liquid phases (both oil and aqueous) and solid phase. Hence, in the absence of the catalyst, the main reaction occurring was hydrothermal pyrolysis of the feedstocks, rather than gasification. The distribution of the feed carbons could be indicative of the pattern of degradability of the feeds under hydrothermal conditions. For instance, mixed waste plastics and RDF retained only 7.42 – 8.65 wt% of their carbon contents in the char products during the non-catalytic tests. On the contrary, the more biogenic samples (mixed waste wood, trommel fines and textile), produced solid residues which retained between 20.9 – 34.2 wt% of feed carbon. However, the carbon contents in the aqueous residuals from all samples were relatively low compared to the other reaction products, possibly due to the extended reaction times, which allowed conversion to oil, gas and solid residues. In the presence of the RuO_2/γ-Al_2O_3 catalyst, there was little or no carbon in the aqueous phases while the distribution of carbon in the oil and char were mostly below 2 wt%, except for MWP, which gave a balance of 6.57 wt% of carbon in the oil product, and MWW with 3.07 wt% carbon in its char product.

The similarity between the MWP and RDF can also be seen from the estimated high yields of oil products in the absence of catalyst (45.1 wt% and 51.5 wt% of carbon balance, respectively), thus giving equally high carbon contents by calculation. Pyrolysis of carbonaceous materials often follows a sequence of moisture loss and devolatilization of organic compounds; however given sufficient time and energy, secondary reactions of the organic volatiles can occur leading to the formation of condensation products, e.g. char [24-26]. Both samples contained mixed plastics, however RDF usually containssome biogenic components such as paper and

8

cardboards as shown in the TGA/DTG profiles (Figure 1). The degradation patterns of biomass and major plastics wastes under TGA conditions are well- known and these can be used to estimate the degradation of the biogenic and plastic fractions of MSW [27]. From Table 1, the C/H mole ratio in MWP is 1/1.78, while in the RDF it is 1/2.04, so that both samples have similar CH_2 empirical formula of polyolefin plastics (especially polyethylene and polypropyelene) which make up a large proportion of waste plastics [26, 28].

Oil production from the two plastic-rich samples could be linked to their TGA/DTG profiles in Figure 1, which show that the loss of their volatile fractions occurred around the reaction temperature used in this work. Hence, in the absence of a catalyst, the volatiles from RDF and MWP would only just be released around the reaction temperature, without sufficient energy for secondary reactions to produce char. For the other three biogenic samples however, their devolatilization occurred at much earlier temperatures compared to the plastic-rich samples. This may explain why the oil yields from MWW and TXT were low, whereas they gave high char and gas yields during the non-catalytic tests. Indeed, in terms of gas yields, MWW and TXT gave the highest carbon gasification efficiency (CGE) during the non-catalytic tests, mainly as carbon dioxide resulting from possible decarboxylation of biomass components and the possible degradation of ester and amide linkages in textile materials. TF was the most complex sample in the set with a large variety of different components, including some biogenic fractions and some components which thermally degraded even at about 750 °C.

3.2. Detailed evaluation of gasification results

3.2.1.Gas compositions

Table 3 presents the volume percents of gas components from the non-catalytic and catalytic tests of the five samples. During the non-catalytic tests, the more biogenic samples (MWW, TXT and TF) produced carbon dioxide as the predominant gas, while MWP and RDF produced more alkane gases. The gas product from MWP from the non-catalytic tests was composed of more hydrocarbon gases (60.1 vol.%) than the RDF sample (43.6 vol%). Additionally, the concentration of CO_2 was higher in the gas product from RDF than that from MWP, which may be due to differences in the composition of the two samples. Table 1 also shows that, the RDF sample contained more oxygen atoms than the MWP. As such, the decomposition of biogenic components would be the likely reason for obtaining more CO_2 from RDF than from MWP. The volume percent of hydrogen gas was highest in the product gas from TF and lowest in the gas product from the textile waste sample. Interestingly, CO was found in appreciable

concentrations in all the gas products; it was lowest in the gas from MWW but with similar concentrations in the gas products from RDF, TF and TXT samples.

During the catalytic experiments with the 20 wt% $RuO_2/\gamma\text{-}Al_2O_3$ catalyst, Table 3 shows that methane and carbon dioxide became the predominant gases, followed by hydrogen gas and a dramatic reduction in the volume percent of $C_2\text{-}C_4$ hydrocarbon gases for all samples. This suggests that the influence of the catalyst may include the cleavage of C-C bonds in the higher alkanes. The volume percent of hydrogen gas was reasonably high and comparable to hydrogen production from the non-catalytic tests. Interestingly, the actual yield of hydrogen gas increased with the ruthenium catalyst, particularly for the highly biogenic TXT, TF and MWW samples, as discussed in Section 3.2.4 below More importantly, there was a total absence of CO in all the gas products in the presence of the catalyst, indicating its conversion either by reduction to methane or oxidation via the water-gas shift reaction, which produced hydrogen.

The calorific value of the gas products obtained from each of the SCWG experiments was calculated using the following formula;

$$Higher\ Heating\ Value\ (HHV), \text{MJ } kg^{-1} = \sum_{i=1}^{n} x.CV$$

where i …n = each combustible component in the gas product
x = mass fraction of gas component produced
CV = calorific value (HHV) of gas component in MJ kg^{-1}

The HHV of the gas products obtained in this work are also presented in Table 3. The results show that during the non-catalytic tests, the calorific values of gas products from the plastic-rich samples (MWP and RDF), were the highest due to the higher yields of $C_2\text{-}C_4$ hydrocarbon gases. Under ruthenium catalysis, overall conversion improved dramatically for all samples and so did the calorific values of the gas products. The much higher yield of hydrogen from the biogenic samples improved the calorific values of their gas products.

3.2.2. Gas yields

The yields of the gas components (in mol kg^{-1} of feedstock) are displayed in Figure 2. Clearly, the total gas yields for the different samples more than doubled in the presence of the catalyst due to increased conversion. Obviously, CGE was much higher during the catalytic tests, with values between 94 wt% and 98.8 wt% for all samples. The RuO$_2$/γ-Al$_2$O$_3$ catalyst was able to convert nearly all the carbon atoms in the different feeds into gas. For the non-catalytic tests, the highest CGE was obtained from the textile wastes, which reached 54 wt%, followed by the mixed waste wood, while the lowest CGE was measured with the TF samples. Interestingly, Figure 2 shows that in the presence of the catalyst, the plastic-rich samples produced more methane than the biogenic samples. Also important of note is the comparison between the yields of carbon dioxide and methane in relation to the two sets of samples. Carbon dioxide was the dominant gas for the biogenic samples, while hydrocarbon gases dominated the gas products from the plastic-rich samples during both catalytic and non-catalytic tests. For instance, the yield of carbon dioxide from MWW was 13.6 mol kg^{-1}, while total hydrocarbon gases yield was 5.22 mol kg^{-1} under non-catalytic conditions. In contrast, the yield of carbon dioxide was only 4.49 mol kg^{-1} from MWP, while combined hydrocarbon gases yield was 11.8 mol kg^{-1} under identical conditions. For the catalytic tests, carbon dioxide yield from MWW was 22.1 mol kg^{-1}, while hydrocarbon gases yield was 18.0 mol kg^{-1}, with methane accounting for nearly 97% of total hydrocarbon gases. In the presence of the catalyst, MWP produced carbon dioxide yield of 25.2 mol kg^{-1} and total hydrocarbon gases yield of 32 mol kg^{-1}, with more than 91% of this as methane.

3.2.3. Carbon selectvity as hydrocarbon gases

The selectivities of the feed-carbon atoms in the carbon-containing gas components in the gas products were calculated according to the following formula;

$$Hydrocarbon\ selectivity, wt\% = \frac{\text{Mass of carbon in a hydrocrabon gas components (g)x 100}}{\sum \text{Mass of carbon in } (CH_4 + CO_2 + CO + (C_2 \ldots + C_4)) \text{ in gas product (g)}}$$

In the absence of the RuO$_2$/γ-Al$_2$O$_3$ catalyst, the combined selectivity for C$_2$-C$_4$ hydrocarbon gases in the gas products were much higher than that of methane in all five samples as shown in Figure 3a. Based on the details of Table 3, it can be seen that RDF and MWP samples

particularly gave gas products with much higher carbon selectivities towards the higher alkanes (ethane, propane and butane) than towards methane in the absence of ruthenium catalysts. The use of the RuO_2/γ-Al_2O_3 catalyst changed the gasification profiles of the samples, leading instead to an opposite trend in the selectivities for the hydrocarbon gases compared to the non-catalytic tests. Figure 3b shows that in the presence of the catalyst, hydrocarbon gas selectivity increased dramatically in favour of methane with corresponding decreases in selectivities towards the C_2-C_4 gases for all samples. The ability of ruthenium catalysts to promote methanation and C-C bond cleavages has been well reported in literature [16-17, 23]. With the RuO_2/γ-Al_2O_3 catalyst, the total selectivity for hydrocarbon gases increased at least twice for all samples, excepting waste textile and MWW compared to values obtained without the catalyst. For instance, for RDF, TF and MWP, hydrocarbon selectivity increased by factors of 2.2, 2.1 and 2.0; while MWW and TXT increased by factors of 1.6 and 1.4, respectively. The general increase in total hydrocarbon selectivities across the range of samples indicated that the RuO_2/γ-Al_2O_3 catalyst was not only able to crack the higher hydrocarbon gases but was able to convert the chars and oil products as well or prevent their formation in favour of methane production.

3.2.4. Hydrogen gasification

The conversion of feedstock hydrogen atoms to gas was also evaluated in this work to support the influence the ruthenium-based catalyst. Hydrogen gasification was calculated according to the equation below;

$$Hydrogen\ gasification, wt\% = \frac{\text{Mass of hydrogen in gas products (g) x 100}}{\text{Mass of hydrogen in the feedstock (g)}}$$

Figure 4 shows the yields of hydrogen atoms in gas components including H_2 and the hydrocarbon gases. The hydrogen yields have been presented as hydrogen in H_2, methane and total hydrogen gasification efficiency (HGE), respectively for the different feedstocks. The HGE has been calculated as the total hydrogen yield in the gas products. Results show that the presence of the RuO_2/γ-Al_2O_3 catalyst led to very large increase in overall hydrogen gasification compared to reactions without the catalyst. In the absence of the catalyst, the hydrogen yields as H_2 and methane were much lower than the HGE values. This showed that $C_2 - C_4$ hydrocarbons accounted for a large proportion of the observed HGE. In contrast, in the presence of the RuO_2/γ-Al_2O_3 catalyst, the yields of hydrogen as H_2 and methane accounted

12

for more 90% of the HGE values, with methane accounting for at least 75% of hydrogen yield in gas products. In addition, the HGE values obtained from the catalytic tests were in all cases greater than 100%, indicating that hydrogen from water contributed to the overall hydrogen gasification. Recently, Zhou et al. [29] reported that a porous nickel catalyst was effective for methane production from cellulose in the presence of Zn, which produced the hydrogen gas required for the methanation reaction by its reaction with water. In other words, water served as the source of hydrogen for the methanation reaction catalysed by the porous nickel catalyst.

3.3. Catalyst stability tests

The stability of the RuO_2/γ-Al_2O_3 catalyst was tested by re-using the same catalyst sample for the gasification of the composite RDF sample in four consecutive runs. The results of these tests are presented in Figure 5, which showed that the catalytic activity changed slightly during the tests, with the noticeable gradual changes in the yields of methane and hydrogen with repeated catalyst use; there was an increase in methane yield at the first time of reusing the catalyst followed by subsequent gradual decrease in methane yields, which corresponded to gradual increases in hydrogen yields. In addition, the CGE values decreased consistently with repeated catalyst use. The fresh as used catalysts were characterized by SEM-EDX. The SEM images show increase in the particle size of the catalyst with repeated use, which could possibly result from agglomeration. This increase in ruthenium particle size was reported by Osada et al. [30] during SCWG of lignin. In addition, the SEM-EDX analyses show the presence of other elements including Si, Fe, Ca, Na and Ti in the reused catalysts (Figure 6). These elements have been confirmed to originate from the RDF sample itself. Hence, with repeated use the catalyst became more and more diluted by the ash contents of the RDF sample, which may cover the catalyst or make the surface of the catalyst inaccessible. Osada et al. [30] and Guan et al. [31] attributed the loss in catalytic activity of ruthenium during SCWG to sulphur poisoning. No sulphur was found in the used catalyst, so that the presence of ash however, may also contribute to the decrease in the overall efficiency of the RuO_2/γ-Al_2O_3 catalyst, in terms of gas yields and CGE.

Of particular importance in this part of the work is the poor gasification results obtained from the used catalysts without re-calcination compared to other results in Figure 5. As shown in the figure, the CGE from the test with the used non-calcined catalyst was only 57.6 wt%. Furthermore, while no CO was produced from the tests with the fresh and used calcined catalyst, the used non-calcined catalyst gave a small yield of CO (0.85 mol kg^{-1}). Though small,

the presence of CO indicated that reactions consuming it were not highly active. In addition, the higher yield of hydrogen and carbon dioxide compared to methane from this test showed that methanation reaction was equally not being promoted. Rather, it would appear that much of the CO produced was consumed via water-gas shift reaction.

To investigate this further, the fresh catalyst, the used non-calcined catalyst residue and the used calcined catalyst were analyzed by X-ray diffraction (XRD) technique. Figure 7 presents the phase patterns in these samples. The fresh catalyst is mainly composed of the RuO_2 and γ-Al_2O_3 as expectedly shown in Figure 7a. The used non-calcined catalyst contained (Figure 7b) phases of γ-Al_2O_3, metallic ruthenium, and phases of other compounds, mainly from the ash contents of RDF. The identified extra compounds included calcium carbonate, calcium silicate, calcium ruthenium oxide, iron(III) oxide and calcium titanium oxide. Only two small peaks could be ascribed to RuO_2 in the used non-calcined catalyst. On calcination of the used catalyst, the RuO_2 peaks re-appeared and no Ru metal peak was observed in Figure 7c. The XRD results are thus in agreement with the SEM-EDX results, which as earlier explained, indicated the presence of elements such as Si, Ca, Ti and Fe.

The two main implications of the XRD and SEM-EDX results are that; (1) they show that after the catalytic SCWG process, the RuO_2 was reduced almost completely to Ru metal; (2) the catalyst became diluted with ash from the RDF samples, which would increase with repeated use of the same catalyst sample. Therefore, these results could explain the significant loss of catalytic activity with the used catalyst without calcination. As would be explained in Section 3.5 (on possible reaction mechanism), these results indicated that the feedstock reforming reaction was initiated by RuO_2 and its reduction to Ru metal led to the loss activity in this particular stage of the catalytic process. The results also show that RuO_2 being a reactive catalyst, could be used in a manner similar to the use of other oxidative catalysts such as V_2O_5 in the sulphuric acid process. Dreher et al. [32] have shown that deactivated (sulphur-poisoned) ruthenium catalysts could be regenerated on-stream using mild oxidation by hydrogen peroxide.

3.4. Effect of catalyst composition
The effect of the catalyst compositions on the SCWG process was investigated in this work using RDF feedstock. These tests were carried out by using 0.8 g of γ-Al_2O_3, 0.2 g of RuO_2 and a mixture of the two oxides (0.2 g RuO_2 and 0.8 g of γ-Al_2O_3) for separate SCWG of 2.0

g of the RDF sample. The results are presented in Figure 8. According to the results, in the presence of only γ-Al_2O_3, the CGE value was only 32.7 wt% which is similar to the CGE value (34.8 wt%) obtained from the non-catalytic test. The gas product obtained in the presence of gamma-alumina contained 18 vol% hydrogen, 13.1 vol% methane, 33.4 vol% carbon dioxide and 24.7 vol% of C_2-C_4 hydrocarbon gases. Interestingly, no carbon monoxide was detected, whereas the non-catalytic test yielded 6.27 vol% of CO. This may indicate that the γ-Al_2O_3 could catalyse the water-gas shift reaction, thus converting CO to hydrogen. Alumina is used as the main support for water-gas shift catalysts, as it has shown to be more effective than other support materials [33]. Apart from the volume percent yields of hydrogen and methane, it would appear that the yields of carbon dioxide and C_2-C_4 hydrocarbons were similar to those obtained from the non-catalytic tests.

In the presence of RuO_2 alone, CGE was 84.6 wt%, which is much higher than the CGE from the tests with γ-Al_2O_3. Clearly, RuO_2 was able to convert more of the carbon contents of the RDF to gas. Figure 8 shows that the yields of all the gas components increased dramatically in the presence of RuO_2. For example, methane yield increased from 1.7 mol kg^{-1} in the presence of γ-Al_2O_3 to 15.2 mol kg^{-1} when RuO_2 was used. With the physically mixed oxides, the CGE further increased to 96.7 wt%, which is similar to the CGE (97.8 wt%) obtained from the SCWG of RDF using the prepared RuO_2/γ-Al_2O_3 catalyst. Compared with RuO_2 alone, the mixed oxides led to a decrease in the yields of C_2-C_4 hydrocarbons, while hydrogen yield remained fairly constant. In contrast, the yields of carbon dioxide and methane increased, with methane increasing much more than carbon dioxide. Indeed, the gas products in the presence of RuO_2 and the mixed oxides contained 12.1 vol% and 7.53 vol% of C_2-C_4 hydrocarbons, respectively compared to 24.7 vol% obtained in the presence of γ-Al_2O_3 alone. These results show that RuO_2 was responsible to the high CGE observed and also for the increased yield of methane. The increased CGE, CO_2 yield, and especially methane yield in the presence of the mixed oxides may thus be due largely to improved dispersion of the RuO_2 on the γ-Al_2O_3 support, rather than any synergistic chemical effect. So that the physical mixing of the oxides led to increased apparent volume of the RuO_2 catalyst and apparent surface area, thus causing improved catalytic activity. Clearly, physical mixing of the two oxides yielded a CGE comparable to the prepared catalyst; however the impregnated RuO_2/γ-Al_2O_3 catalyst produced higher yields of methane and lower C_2-C_4 hydrocarbon, obviously due to better catalyst dispersion. Physical observation of the mixed oxides catalyst after the experiments showed some morphological differences. The mixture had virtually separated into white patches of

alumina and dark patches of possible ruthenium species, respectively on a filter paper, whereas the prepared catalysts maintained its homogeneous dark colour.
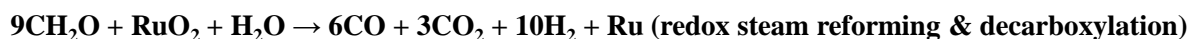
3.5. Possible reaction mechanisms

The high CGE observed in the presence of the RuO_2/γ-Al_2O_3 catalyst showed clearly that the catalyst, particularly the RuO_2, promoted the conversion of all gasifiable forms (solid, liquid and gas) of the samples into gas. Importantly, the yields of C_2-C_4 hydrocarbons decreased while the yields of methane and carbon dioxide increased compared to results from non-catalytic tests (Table 3). Hence, the catalyst must be promoting reactions leading to the formation of these products. The increased yield of hydrogen and carbon dioxide as well as the corresponding disappearance of CO, suggest the occurrence of water-gas shift reaction. At the same time, the higher yields of methane from the biogenic samples, especially the MWW sample, may indicate that methanation of CO or CO_2 also occurred and was catalysed by the ruthenium component of the catalyst. Particularly for the plastic-rich samples, the formation of methane could be attributed directly to hydrogenolysis of the C-C hydrocarbon chains. However, the increased yield of carbon dioxide from the plastic-rich samples also showed that carbon reforming occurred via RuO_2 catalysis.

Park et al. [11] proposed a catalytic mechanism for SCWG of glucose and cellulose, involving steam reforming and methanation under RuO_2 catalysis. The results of this work agree with this mechanism, especially for the biogenic samples. In addition, the plastic rich samples also exhibited a mechanism involving C-C bond cleavage and hydrogenation as well as steam reforming and methanation. Although, Park et al. [11] reported that the catalytic reaction of ruthenium involved a Ru^{IV} and Ru^{II} redox cycle, no Ru^{II} was observed in this work. In addition, RuO or $Ru(OH)_2$, which are the possible forms of ruthenium in aqueous environments are unstable or non-existent [34]. For example, RuO, if at all only exists as a gas at temperatures around 1630 °C [35], which is far above the temperature used in this work. However, elemental Ru (Ru^0) was found in the solid residues (analysed without calcination) from this work; thus indicating that the ruthenium catalysis redox cycle involved Ru^{IV} and Ru^0 Furthermore, literature has shown that elemental ruthenium is an excellent catalyst for methanation reactions [36-37]. Hence, on the basis of the results obtained from this work, the possible reaction mechanisms for the SCWG of the biogenic and plastic-rich samples have been proposed based on the stoichiometric reactions below;

Scheme 1: Biogenic samples

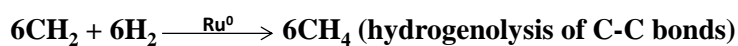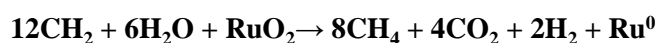*Decarboxylation, steam reforming, direct hydrogenolysis and methanation*

$9CH_2O + RuO_2 + H_2O \rightarrow 6CO + 3CO_2 + 10H_2 + Ru$ (redox steam reforming & decarboxylation)

$6CO + 6H_2O \rightarrow 6CO_2 + 6H_2$ (water-gas shift reaction)

$3CH_2O + 6H_2 \xrightarrow{\quad Ru^0 \quad} 3CH_4 + 3H_2O$ (direct hydrogenolysis)

$2CO_2 + 8H_2 \xrightarrow{\quad Ru^0 \quad} 2CH_4 + 4H_2O$ (methanation)

Overall

$12CH_2O + RuO_2 \rightarrow 5CH_4 + 7CO_2 + 2H_2 + Ru$

Scheme 2: Plastic-rich samples

Steam reforming, methanation and direct hydrogenolysis

$6CH_2 + RuO_2 + 4H_2O \rightarrow 6CO + 10H_2 + Ru^0$ (redox steam reforming)

$6CO + 6H_2O \rightarrow 6CO_2 + 6H_2$ (water-gas shift reaction)

$6CH_2 + 6H_2 \xrightarrow{\quad Ru^0 \quad} 6CH_4$ (hydrogenolysis of C-C bonds)

$2CO_2 + 8H_2 \xrightarrow{\quad Ru^0 \quad} 2CH_4 + 4H_2O$ (methanation)

Overall

$12CH_2 + 6H_2O + RuO_2 \rightarrow 8CH_4 + 4CO_2 + 2H_2 + Ru^0$

The exact sequence of the above reactions would be an interesting subject for further research but an attempt would be made in this paper. For instance, since little or no CO was observed in all the catalytic tests, it could be suggested that water-gas shift was possibly the fastest reaction step under the conditions studied. In this case, it would appear that methane was produced from hydrogen gas reduction of CO_2 (methanation) under ruthenium oxide catalysis. Clearly, formation of carbon dioxide from hydrocarbons such as hexadecane requires an oxidation step, which justifies the redox reaction involving RuO_2 and supercritical water. In contrast, CO_2 production from biogenic samples can readily occur via decarboxylation, with water contributing to the reforming [38-39] of the decarboxylation residues. Considering the results from the catalyst stability tests, the increased yield of hydrogen, the decreased yield of methane and the fairly stable yield of CO_2 with repeated calcination and reuse of the catalyst, all support the possible formation of hydrogen before methane. As such, the loss of catalytic

activity with the reuse of calcined catalyst could correspond to reduced methanation rate while reforming (hydrogen production) was largely unaffected. As stated before, for the non-calcined catalyst, the significant loss in catalytic activity was mostly due to the presence of Ru rather than the oxidative RuO_2, which was responsible for the initial steam reforming stage.

To further support these possible mechanisms, two model compounds, (glucose, for biogenic samples and n-hexadecane, for plastic-rich, long-chain hydrocarbon), were reacted separately at 450 °C for 10 min and 60 min, respectively. The gas yields and CGE for the two samples are shown in Figure 9. Rather surprisingly, the gas products obtained from n-hexadecane after 10 min contained very little C_2-C_4 hydrocarbons, which may indicate the suppression of pyrolysis in the presence of the RuO_2 catalyst. Even at 10 min, n-hexadecane produced hydrogen, methane and carbon dioxide, with more hydrogen than methane. However, after 60 min, methane yield increased dramatically and became much higher than the yields of hydrogen and carbon dioxide, which supports the methanation and direct hydrogenolysis mechanisms. In addition, glucose produced more carbon dioxide than methane under both reaction times, supporting the decarboxylation mechanism in biogenic samples. The production of substantial yield of hydrogen after just 10 min would be evidence of steam reforming reactions of the carbonaceous materials. Steam reforming and water-gas shift reactions represent the net contribution of hydrogen from water to the hydrogen yields during SCWG such that more than 100% HGE was realized for all samples. HGE values were higher for the plastic-rich samples compared to the biogenic samples, possibly because much of the carbon atoms in the plastic-rich samples participated in steam reforming reactions for hydrogen production. In contrast, some of the carbon atoms in the biogenic samples were lost via decarboxylation. Hence, the nature of covalent bonds in the carbonaceous material may be an important factor for gasification products.

4.0. Conclusions

Supercritical water gasification of RDF and its components have been carried out with and without 20 wt% RuO_2/γ-Al_2O_3 catalyst at 450 °C for a reaction time of 60 min. The tests provided new insights into the catalytic reaction of RuO_2 during SCWG of carbonaceous materials. Without the catalyst, CGE ranged from 35 wt% to 54 wt%, with TF and TXT samples giving the lowest and highest values, respectively. The non-catalytic tests of the plastic-rich samples (RDF and MWP) produced mainly liquid oils and high yields of hydrocarbon gases due to pyrolysis. The biogenic samples (MWW, TXT and TF) gave high

18

yields of char and carbon dioxide in the gas products without the catalyst. The presence of the $RuO_2/\gamma\text{-}Al_2O_3$ catalyst led to increased CGE for the five samples, ranging from 94 wt% to 99 wt%. In addition, the catalyst dramatically increased yields of methane, and hydrogen and carbon dioxide. The use of model compounds (glucose for biogenic samples and hexadecane for plastic rich samples) and detailed evaluation of results of the analyses of solid residues revealed the possible reaction mechanisms for the two sets of samples during catalytic SCWG. For both sets of samples, their conversions appeared to have involved mainly steam reforming, direct hydrogenolysis and methanation. In addition, the conversion of the biogenic samples could involve some decarboxylation mechanism. The increased yields of both a reduction product (methane) and an oxidation product (CO_2) suggest that the $RuO_2/\gamma\text{-}Al_2O_3$ catalyst may be involved in a redox-type catalytic mechanism, possibly involving Ru^{IV} and Ru^0. The reduction of Ru^{IV} to Ru^0 was necessary for the overall SCWG process; however the catalytic process required re-oxidation of Ru^0 to Ru^{IV}. There appeared to be some synergistic effects of alumina and RuO_2, which led to increased CGE but this may only relate to the improved dispersion of the RuO_2 on the alumina support.

5.0 References

[1] A. Garg, R. Smith, D. Hill, N. Simms, S. Pollard, Environm. Sc. Technol., 2007, **41,** 4868-4874.

[2] A. Garg, R. Smith, D. Hill, P. J. Longhurst, S. J. Pollard, N. J. Simms, Waste Manage., 2009 **29,** 2289-97.

[3] P. T. Williams, Waste Treatment and Disposal, 2005. Chichester, England, John Wiley & Sons

[4] X. Xu, M.J. Antal, Jr., Environ. Progress, 1998, **17**, 215 - 220

[5] X. Xu, Y. Matsumura, J. Stenberg, M.J. Antal, Jr., Ind. Eng. Chem. Res. 1996, **35**, 2522 - 2530

[6] D. C. Elliott, G.G. Neuenschwander, M.R. Phelps, T.R. Hart, A.H. Zacher, L.J. Silva, Ind. Eng. Chem. Res. 1999, **38**, 879 - 883

[7] D. C. Elliott, M. R. Phelps, L. J. Sealock, Jr., E. G. C. Baker, Ind. Eng. Chem. Res., 1994, 33, 566 – 574

[8] A. Sinag, A. Kruse, Schwarzkopf, Eng. Life. Sci., 2003, 3, 469-473

[9] J. A. Onwudili, P. T. Williams, Int. J. Hydrogen Energy, 2009, **34**, 5645-5656

[10] B. Kuhlmann, E. M. Arnett, M. Siskin, J. Org. Chem. 1994, **59**, 3098-3101

[11] K. C. Park, H. Tomiyasu: Chem. Comm., 2003, **6**, 694 – 695

[12] Y. Liu, H. Kang, X. Gong, L. Jiang, Y. Liu, S. Wu, RSC Adv. 2014,**4**, 22367-22373

[13] S. Lin, Y. Suzuki, H. Hatano, M. Harada, *Kagaku Kogaku Ronbunshu*, 1999, **25**, 498-501.

[14] S. Lin, M. Harada, Y. Suzuki, H. Hatano, *Kagaku Kogaku Ronbunshu*, 2002, **28**, 626-630.

[15] Y. M. Gong, S. Z. Wang, X. Y. Tang, Adv. Mat. Res., 2014, **1010-1012**, 952-955, Aug. 2014

[16] A. J. Byrd, K. K. Pant, R. B. Gupta, Ind. Eng. Chem. Res., 2007, **46**, 3574-3579.

[17] D. T. Yamamura, T. Mori, K. C. Park, Y. Fujii, H. Tomiyasu, J. Supercritical Fluids, 2009, **51**, 43–49

[18] T. Sato, M. Osada, M. Watanabe, M. Shirai, K. Arai, Ind. Eng. Chem. Res., 2003, **42**, 4277-4282.

[19] L. Chen, Y. Zhu, H. Zheng, C. Zhang, B. Zhang, Y. Li, J. Mol. Cat. A: Chemical, 2011, **351**, 217-227

[20] J. A. Onwudili, Biores. Technol. 2015, **187**, 60-69

[21] J. A. Onwudili, P. T. Williams, Green Chem. 2014, **16**, 4740-4748

[22] J.A. Onwudili and P. T. Williams, Appl. Cat. B: Environ. 2016, **180**, 559-568

[23] Y. Karakus, F. Aynaci, E. Kipçak, M. Akgün, Int. J. Hydrogen Energy, 2013, **38**, 7298-7306

[24] N. Shah, J. Rockwell, G.P. Huffman, Energy & Fuels, 1999, **13**, 832-838

[25] Lee, K.-H. and D.-H. Shin, Waste Manage. 2007, **27** 168-176.

[26] C. Muhammad, J. A. Onwudili, P. T. Williams, Energy & Fuels, 2015, **29**, 2601-2609

[27] E. C. Efika, J. A. Onwudili, P. T. Williams, J. Anal. Appl. Pyrolysis, 2015, **112**, 14–22

[28] M. Brebu, T. Bhaskar, K. Murai, A. Muto,Y. Sakata,M. A. Uddin, Fuel 2004, **83**, 2021−2028.

[29] Z. Huo, F. Jin, App. Catal. A: Gen. 2015, **490**, 36-41

[30] M. Osada, O. Sato, K. Arai, M. Shirai, Energy & Fuels 2006; **20,** 2337-2343

[31] Q. Guan, C. Wei, P. Ning, S. Tian, J. Gu, Proc Environ. Sci. 2013, **18,** 844 – 848

[32] M. Dreher, M. Steib, M. Nachtegaal, J. Wambach, F. Vogel, ChemCatChem, 2014, **6,** 626-633

[33] J. R. Ladebeck and J. P. Wagner, Catalyst development for water-gas shift. In: W. Vielstich, A. Lamm, and H.A. Gasteiger (eds.), Handbook of Fuel Cells – Fundamentals, Technology and Applications, 2003, **3**, 190–201.

[34] W. E. Bell, M. Tagami, J. Phys. Chem., 1963, **67**, 2432-2436

[35] B. Eichler, F. Zude, W. Fan, N. Trautmann, G. Herrmann, Radiochim. Acta, 1992, **56**, 133-140

[36] F. Solymosi, A. Erdöhelyi, M. Kocsi, J. Chern. Soc. Faraday Trans. I, 1981, **77**, 1003-1012

[37] S. Hwang, J. Lee, U. G. Hong, J. H. Baik, D. J. Koh, H. Lim, I. K. Song, J. Ind. Eng. Chem. 2013, **19**, 698–703

[38] F. Jin, H. Enomoto., Energy Environ. Sci., 2011, **4**, 382-397

[39] A. Kruse, E. Dinjus, Angew. Chem., Int. Ed., 2003, **42**, 909–911

Table 1: Characteristics of the MSW Components used in this work

	Trommel fines (TF)	Textile (TXT)	Refuse derived fuel (RDF)	Mixed waste plastic (MWP)	Mixed waste wood (MWW)
No. of individual items	>30	6	18	21	4
Proximate composition (wt.%)[a]					
Moisture	8.31	4.58	2.01	nd	8.76
Volatile matter	44.5	78.9	83.7	89.5	69.5
Fixed Carbon	0.19	11.8	5.75	4.47	17.8
Ash	47.0	4.70	8.59	6.04	3.95
Ultimate composition (wt.%)[b]					
Nitrogen	1.46	0.63	0.91	0.47	3.29
Carbon	52.7	48.2	73.4	80.5	51.3
Hydrogen	4.77	6.65	12.5	12.0	7.18
Sulphur	0.25	0.04	nd	nd	0.02
*Oxygen	40.8	44.5	13.2	7.01	38.3

a = as received basis; b = dry-ash-free basis; *= by difference

Table 2: Normalized carbon balances during SCWG of MSW components at 450 °C, 60 min

Without catalyst				
Samples	Gas (wt%)	Char (wt%)	Water (wt%)	*Oil (wt%)
Trommel fines	34.8	34.2	0.12	30.9
Textiles	54.0	20.9	2.66	22.4
RDF	34.8	8.65	3.09	53.4
Mixed waste plastics	42.2	7.42	0.53	49.9
Mixed waste wood	52.3	30.2	2.11	15.4

With RuO_2/gamma-Al_2O_3 catalyst				
Sample	Gas (wt%)	Char (wt%)	Water (wt%)	Oil (wt%)
Trommel fines	98.8	<0.01	0.01	1.23
Textiles	97.8	0.95	<0.01	1.25
RDF	97.8	1.79	0.02	0.43
Mixed waste plastics	93.4	<0.01	<0.01	6.57
Mixed waste wood	95.7	3.07	0.04	1.21

* By difference

Table 3: Normalised (nitrogen-free) volume percentage of gas components and HHV of the gas products from SCWG of MSW at 450 °C, 60 min

No Catalyst					
Gas Component (vol.%)	Trommel fines	Textiles	RDF	Mixed waste plastics	Waste wood
Hydrogen	19.5	13.7	13.9	17.6	14.0
Carbon monoxide	5.57	6.04	6.27	4.01	2.35
Carbon dioxide	49.5	57.1	36.3	18.2	56.5
Methane	11.6	15.4	17.0	18.4	18.4
Ethene	0.76	0.24	1.60	1.86	0.17
Ethane	4.41	3.93	9.04	14.7	4.12
Propene	0.81	0.21	1.28	2.74	0.61
Propane	4.84	2.03	10.1	15.3	1.9
Butene & Butadiene	1.20	0.19	3.26	4.12	1.07
Butane	1.80	1.22	1.23	3.03	0.90
Total C$_2$-C$_4$ hydrocarbons	**13.8**	**7.81**	**26.5**	**41.7**	**8.8**
HHV (MJ kg^{-1})	**14.6**	**17.0**	**19.4**	**23.9**	**18.7**

| With RuO$_2$/gamma-Al$_2$O$_3$ catalyst					
Gas Component (vol.%)	Trommel fines	Textiles	RDF	Mixed waste plastics	Waste wood
Hydrogen	15.0	20.9	8.71	13.9	9.66
Carbon monoxide	nd	nd	nd	nd	nd
Carbon dioxide	42.0	46.7	38.2	31.9	44.6
Methane	41.8	30.0	48.7	48.4	44.3
Ethene	nd	nd	nd	0.07	nd
Ethane	0.79	1.47	1.95	2.68	0.96
Propene	nd	nd	nd	nd	nd
Propane	0.39	0.72	1.47	2.30	0.39
Butene & Butadiene	nd	nd	nd	0.25	nd
Butane	0.08	0.24	0.97	0.55	0.12
Total C$_2$ -C$_4$ hydrocarbons	**1.26**	**2.42**	**4.38**	**5.86**	**1.47**
HHV (MJ kg^{-1})	**44.5**	**46.5**	**40.7**	**46.2**	**37.4**

nd = not detected
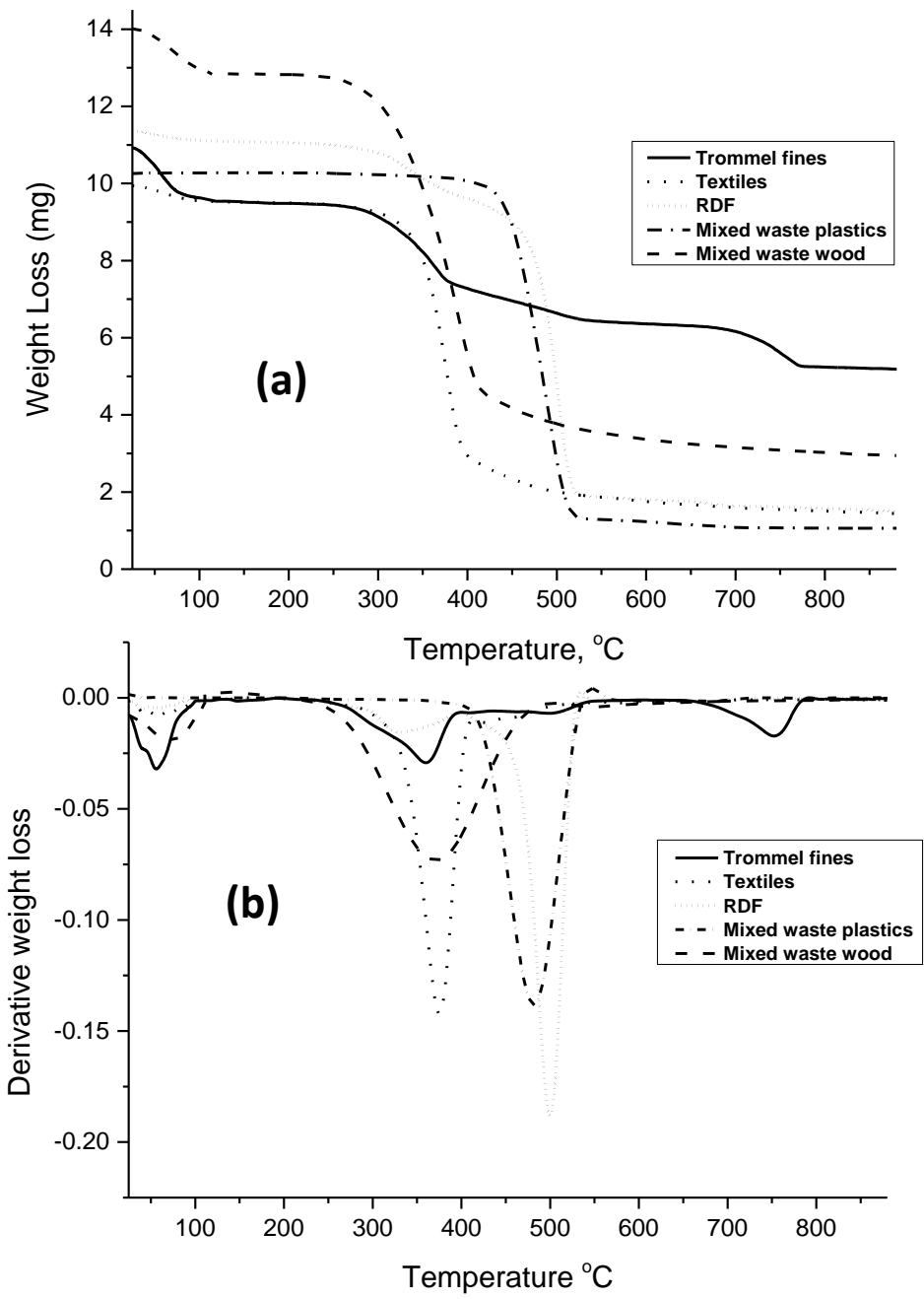
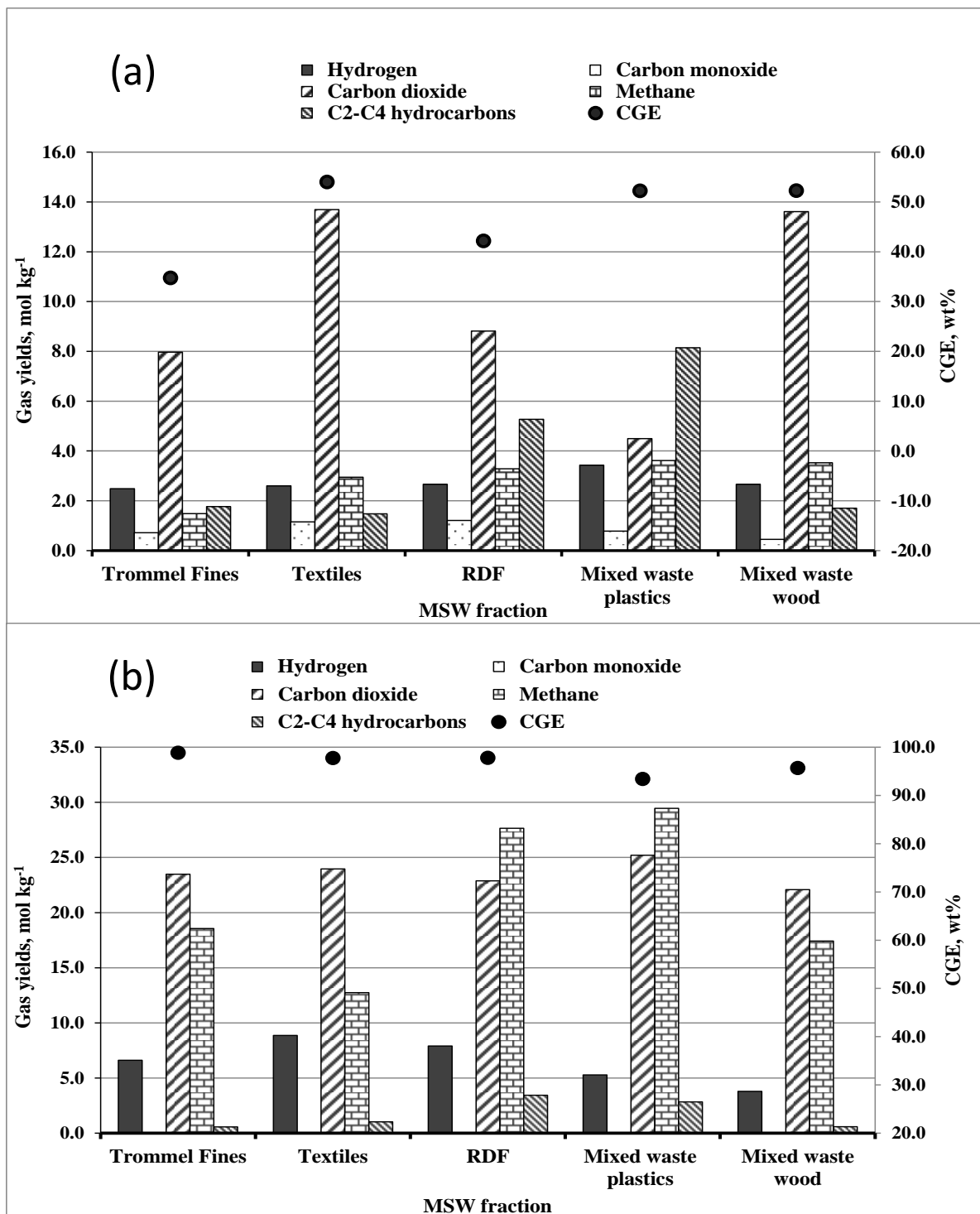Figure 1: TGA/DTG profiles of the MSW fractions

Figure 2: Gas yields from the non-catalytic (a) and catalytic (b) SCWG of RDF components at 450 °C, 60 min
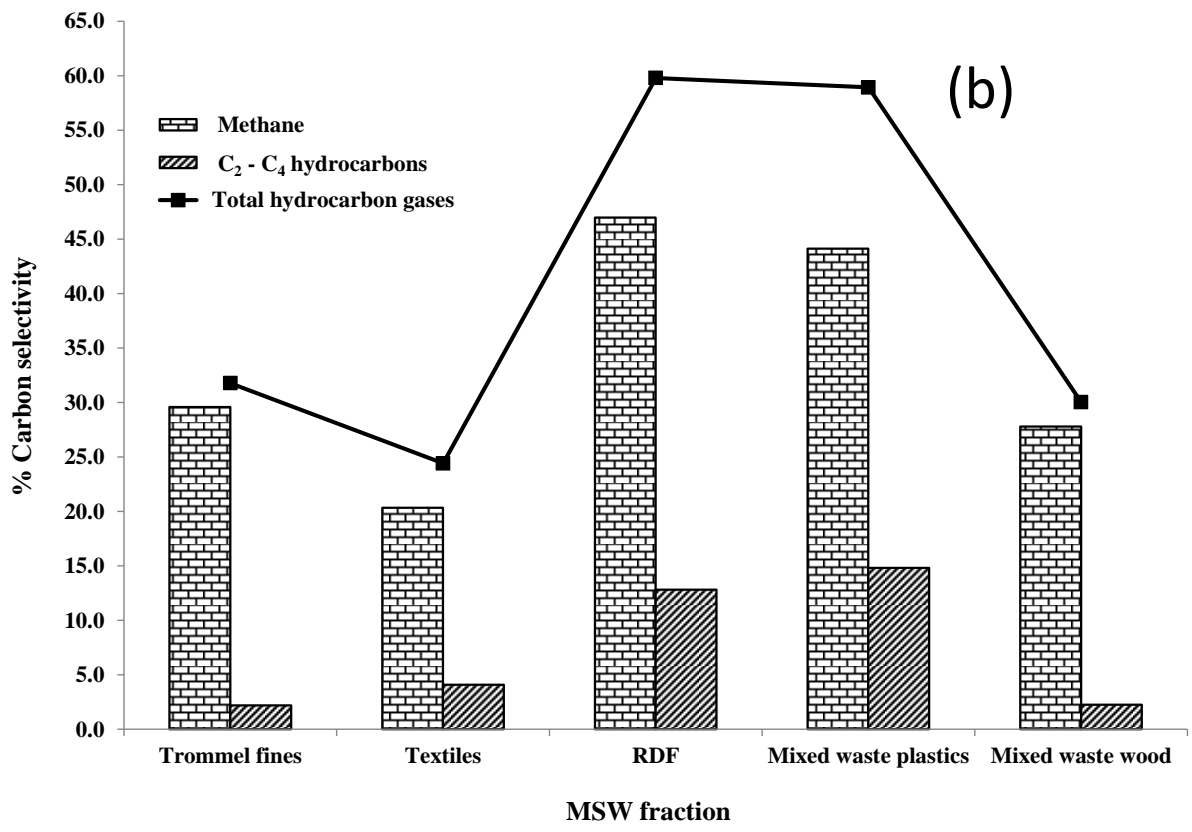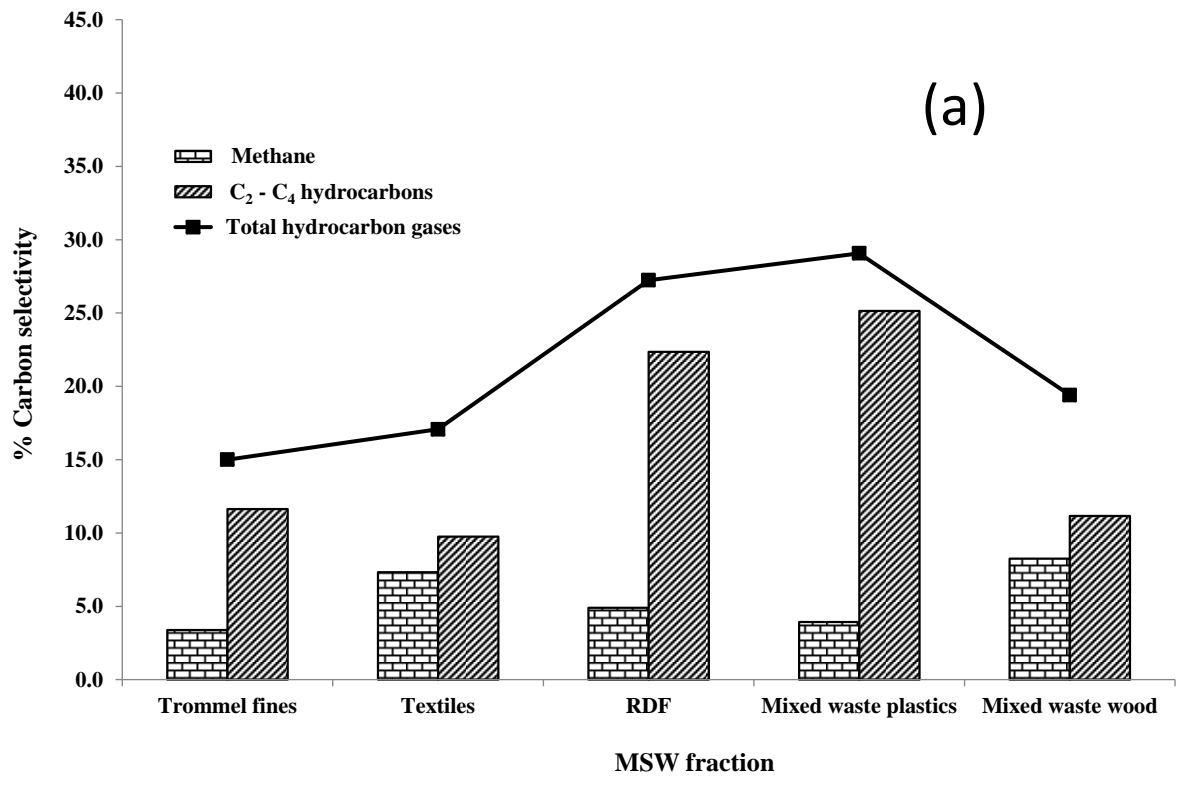
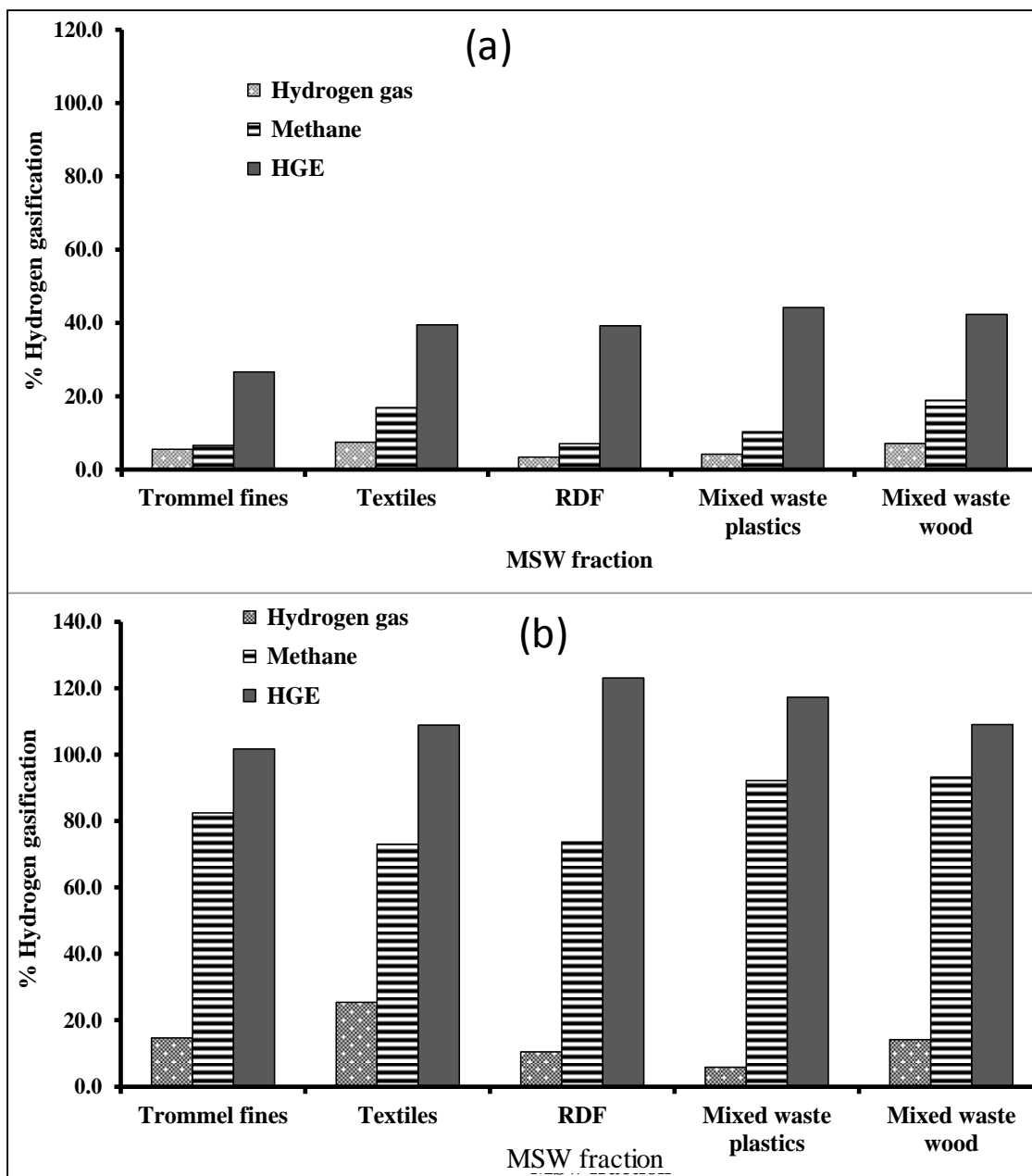Figure 3: Carbon selectivity as hydrocarbon gases from the SCWG of MSW fractions at 450 °C, 60 min (a) non-catalytic (b) with RuO_2/γ-Al_2O_3

Figure 4: Hydrogen selectivity during SCWG of MSW fractions at 450 °C, 60 min; (a) non-catalytic (b) with $RuO_2/\gamma-Al_2O_3$
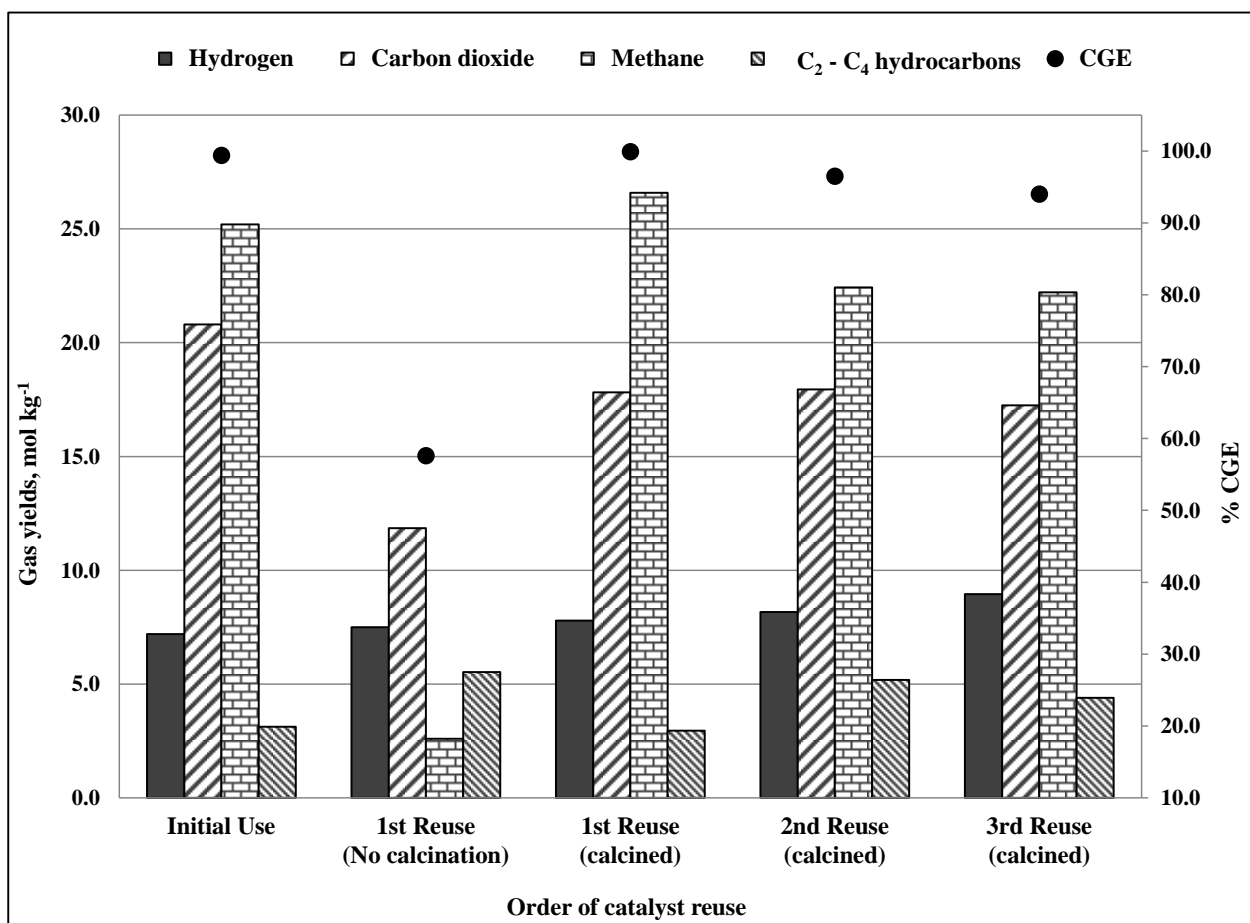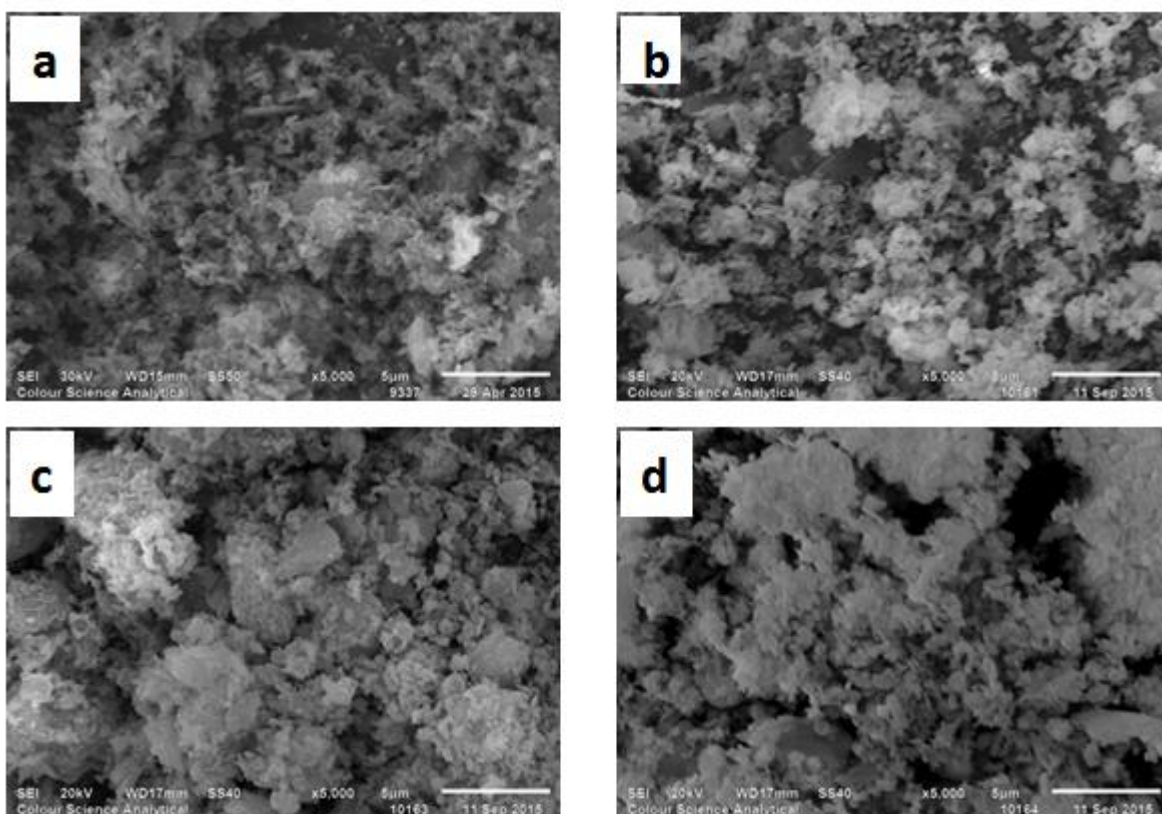
Figure 5: Catalyst stability tests during SCWG of MSW fractions at 450 °C, 60 min

EDX semi-quantitative analysis of fresh and used calcined catalysts

Elements (wt%)	Fresh Catalyst (a)	1st Use (b)	1st Reuse (c)	3rd Reuse (d)
Ruthenium	15.1	14.9	13.8	12.4
Aluminium	33.1	25.4	28.5	26.0
Oxygen	51.8	52.6	43.7	51.6
Silicon	-	1.64	1.15	1.06
Calcium	-	5.50	6.20	6.33
Titanium	-	-	4.41	1.20
Iron	-	-	2.22	1.39

Figure 6: SEM-EDX micrographs of the catalyst and calcined catalyst residues; (a) Fresh $RuO_2/\gamma\text{-}Al_2O_3$ (b) After 1st use (c) After 1st reuse (d) After 3rd reuse
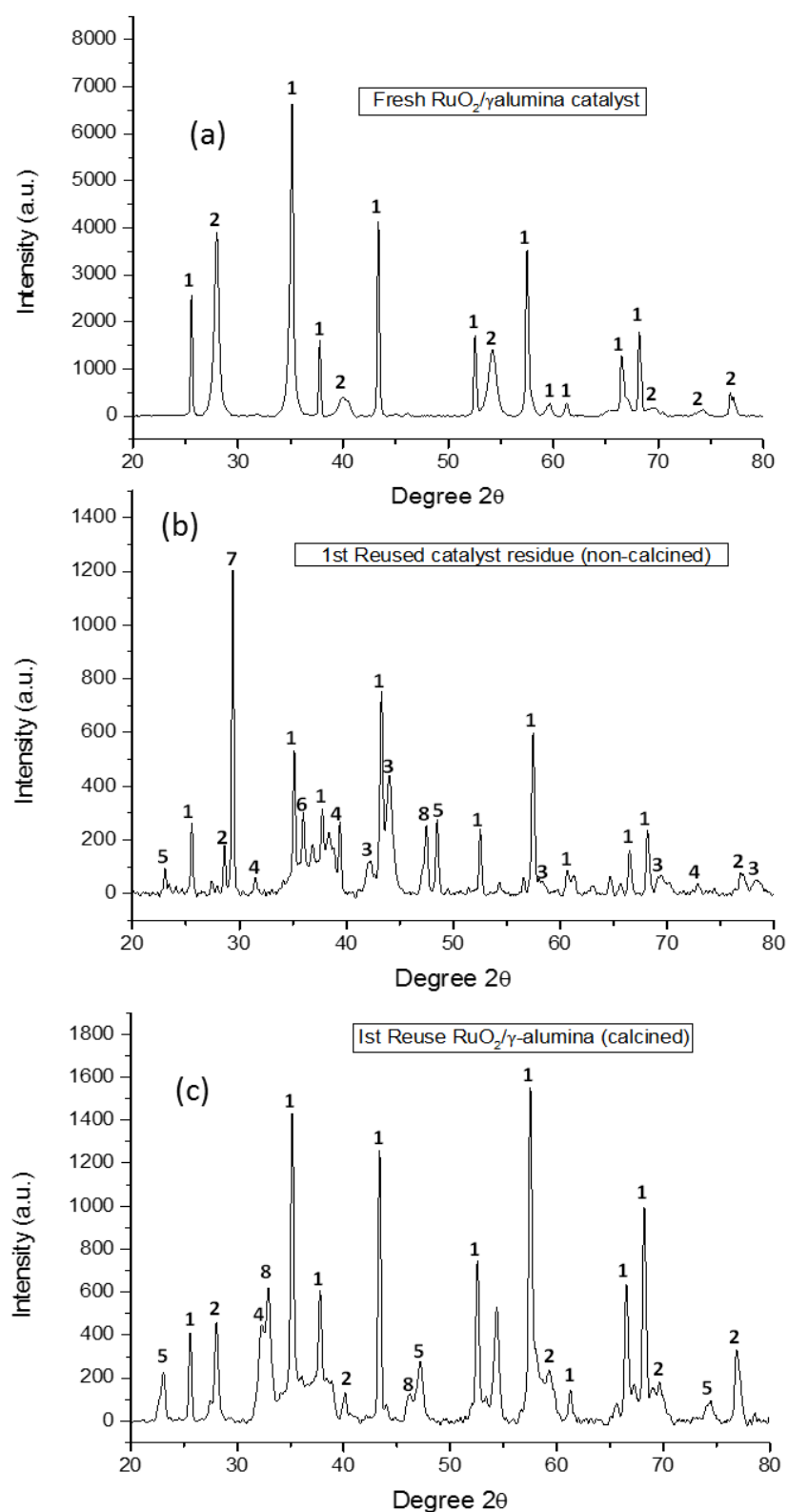
Figure 7: XRD patterns of the catalyst and catalyst residues; **(Top)** Fresh catalyst **(Middle)** non-calcined after 1st reuse **(Bottom)** calcined after 1st reuse. **Peaks: (1)** γ-Al_2O_3; **(2)** RuO_2; **(3)** Ru **(4)** $CaSiO_3$; **(5)** $CaRuO_3$; **(6)** Fe_2O_3; **(7)** $CaCO_3$; **(8)** $CaTiO_3$
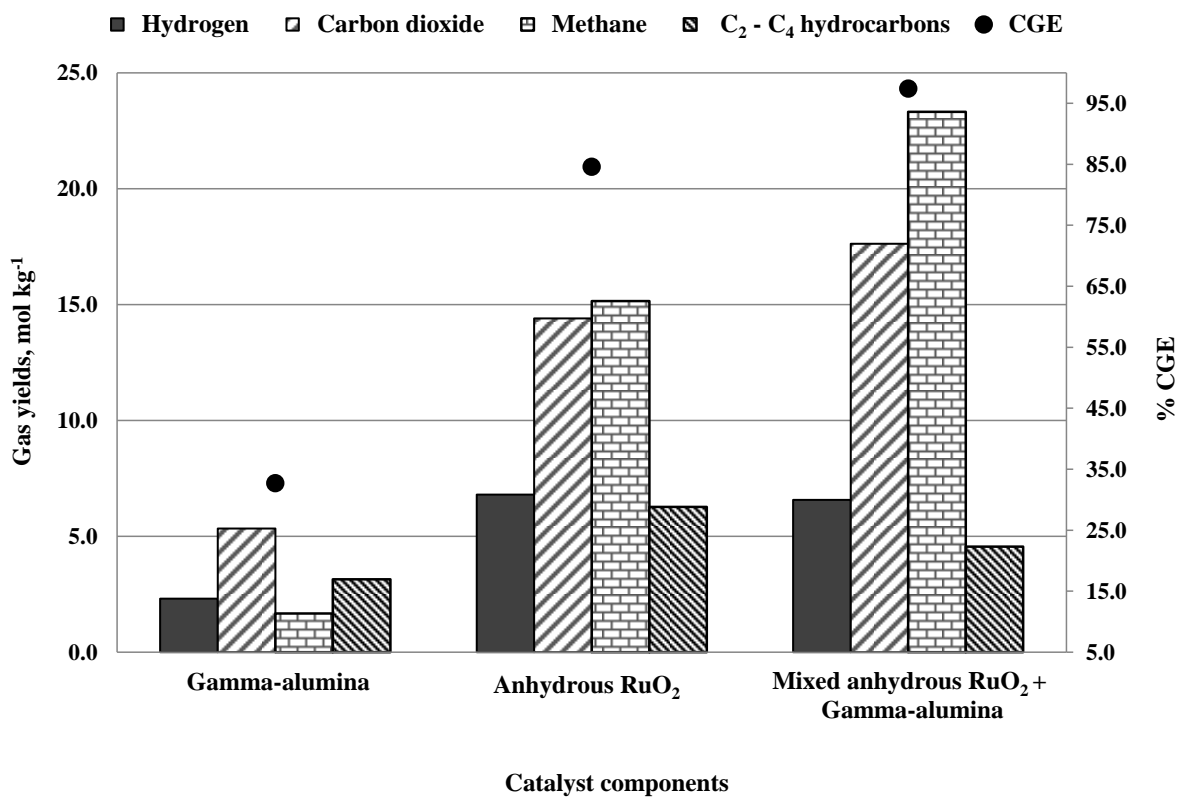
Figure 8: Effects of catalyst compositions on gasification yields of MSW fractions at 450 °C, 60 min; (a) γ-Al₂O₃ (b) anhydrous RuO₂ (c) mixed oxides (0.2 g anhydrous RuO₂ and 0.8 g γ-Al₂O₃)
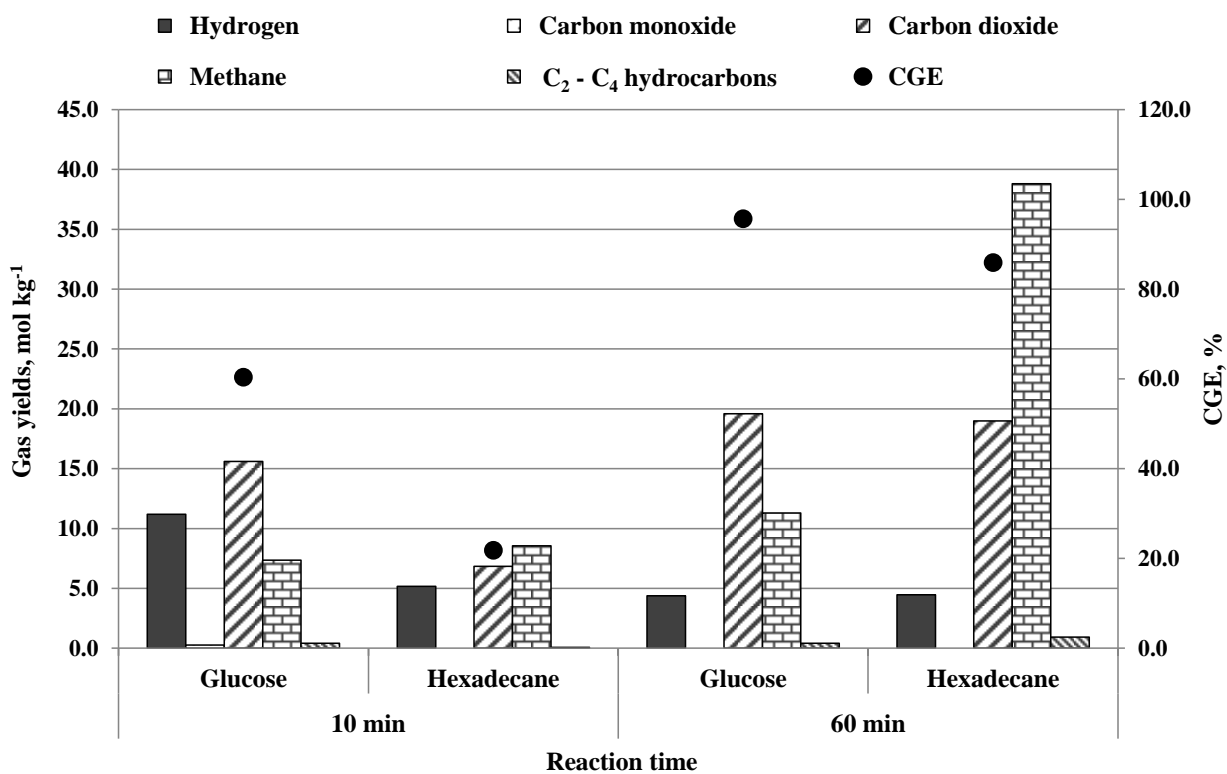
Figure 9: Gas yields from the SCWG of hexadecane and glucose in relation to reaction time at 450 °C; (a) 10 min (b) 60 min